## Journal of Paleontology

## www.cambridge.org/jpa

## **Articles**

Cite this article: Reynolds R.W., Wong Hearing T.W., Williams M., Harvey T., Yanagihara A., Murdock D., Repetski J., Loch J., Lunt D.J., and Gostling N.J. 2025. A new exceptionally preserved phosphatocopid crustacean from the Furongian of Laurentia and a synthesis of Cambrian phosphatocopid distribution patterns. *Journal of Paleontology*, 1–14 https://doi.org/10.1017/jpa.2025.10180

Received: 02 June 2025 Revised: 25 July 2025 Accepted: 29 July 2025

## **Corresponding author:**

Rhicert William Reynolds; Email: rhicert.reynolds@plymouth.ac.uk

**Handling Editor:** Olev Vinn

© The Author(s), 2025. Published by Cambridge University Press on behalf of Paleontological Society. This is an Open Access article, distributed under the terms of the Creative Commons Attribution licence (http://creativecommons.org/licenses/by/4.0), which permits unrestricted re-use, distribution and reproduction, provided the original article is properly cited.





## A new exceptionally preserved phosphatocopid crustacean from the Furongian of Laurentia and a synthesis of Cambrian phosphatocopid distribution patterns

Rhicert William Reynolds<sup>1,2</sup>, Thomas W. Wong Hearing<sup>3</sup>, Mark Williams<sup>3</sup>, Thomas Harvey<sup>3</sup>, Ayari Yanagihara<sup>3,4</sup>, Duncan Murdock<sup>5</sup>, John Repetski<sup>6</sup>, James Loch<sup>7</sup>, Daniel J. Lunt<sup>8</sup> and Neil J. Gostling<sup>2</sup>

<sup>1</sup>School of Geography, Earth and Environmental Sciences, Portland Square, University of Plymouth, PL4 8AA, UK
<sup>2</sup>School of Biological Sciences, Life Sciences Building (Building 85), Highfield Campus, University of Southampton, SO17 1BJ, UK
<sup>3</sup>School of Geography, Geology and the Environment, University of Leicester, University Road, Leicester, LE1 7RH, UK
<sup>4</sup>Faculty of Advanced Science and Technology, Kumamoto University, 2-39-1, Kurokami, Chuo-ku, Kumamoto 860-8555, Japan
<sup>5</sup>Oxford University Museum of Natural History, Parks Road, Oxford, OX1 3PW, UK

## **Abstract**

Planamandibulus nevadensis n. gen n. sp. is a newly discovered exceptionally preserved Laurentian phosphatocopid crustacean described from the upper Windfall Formation (Furongian, Stage 10) in Nevada. Planamandibulus nevadensis has closest affinity with the Baltic and Avalonian taxon Cyclotron. Its occurrence in sedimentary facies associated with dysoxia on the Laurentian paleocontinent fills in a gap in the global distribution of phosphatocopid crustaceans, facilitating a paleoenvironmental synthesis of this Cambrian group. We assess 75 taxa from nine paleocontinental areas spanning Cambrian stages 3 to 10 (~521-486.9 Ma). Comparison of these data with paleoclimate model simulations suggests that phosphatocopid distribution is explained partly by biogeography and ocean temperature patterns. Dabashanella species (e.g., D. hemicyclica Huo et al., 1983) are found across the low paleolatitude (<35°) paleocontinents of East Gondwanan (Australia), South China, and the central Asian terranes, spanning marine shelf carbonates to deeper marine black shale lithofacies, but are absent from mid- and high-paleolatitude sites, suggesting a warmer water preference. A similar warm-water preference is inferred for endemic taxa (e.g., Ulopsis, Parashergoldopsis) of East Gondwana, and perhaps for the newly described Laurentian Planamandibulus. By contrast, the mid- to high-paleolatitude paleocontinents Baltica and Avalonia are characterized by Veldotron, Cyclotron, Bidimorpha, Waldoria, Vestrogothia, Falites, and Trapezilites species, which occur in deep-shelf, cooler-water settings, typically below storm wave base. Hesslandona species sensu lato occur in mid-depth (likely above storm-wave base) warm tropical marine waters but are more typically found in deeper shelf and cooler waters in mid to high paleolatitudes. Phosphatocopids are also associated with sedimentary deposits characteristic of low environmental oxygen concentrations; this is emphasized by a peak in occurrences in the Guzhangian (Miaolingian) and Paibian (Furongian) stages, around the interval of the Steptoean Positive Carbon Isotope Excursion (SPICE) and its associated expansion of anoxic water masses onto shallow marine shelves. Our data compilation and data-model comparison support the environmental preference of phosphatocopids for low-oxygen, but not anoxic, water masses, and the new occurrence of *Planamandibulus* is consistent with this pattern.

UUID: http://zoobank.org/f136f8bf-1ccf-46b0-8980-b88be8f9603d

#### Non-technical Summary

Phosphatocopids are tiny (millimeter-scale) arthropods—animals with jointed limbs, such as crustaceans—that had a global distribution in marine environments during the Cambrian, between about 521 and 487 million years ago. Phosphatocopids are often known only from fossils of the carapace that covered the animal's body, but sometimes exceptionally preserved specimens show soft-anatomical details, as with the new species we describe here from rocks of late Cambrian age in Nevada, USA. The new specimen preserves most of the limbs and some of the body, enabling a very detailed description of an arthropod that lived about 490 million years ago. Phosphatocopids seem to have thrived in marine habitats where oxygen was limited. Their global distribution patterns for the Cambrian are examined here and show that both geography and sea temperature exerted a strong control on their distribution, in a similar manner to many living marine arthropods.

<sup>&</sup>lt;sup>6</sup>United States Geological Survey (USGS)-Emeritus, 12201 Sunrise Valley Drive, Reston, VA 20192, USA

 $<sup>^7\</sup>mathrm{Department}$  of Physical Sciences, University of Central Missouri, Warrensburg, MO 640093, USA

 $<sup>^8\</sup>mathrm{School}$  of Geographical Sciences, University of Bristol, University Road, Bristol, BS8 1SS, UK

#### Introduction

Phosphatocopids are small bivalved and univalved pancrustaceans known from Cambrian strata worldwide (Olempska et al., 2019) that briefly became a significant component of the arthropod micro-benthos during the latest Miaolingian and early Furongian (Olempska and Chauffe, 1999). Phosphatocopids are known predominantly from fossils of their carapaces, although instances of exceptional "Orsten-type" preservation mean they are one of the best-known groups of Cambrian arthropods. Although this secondary phosphatization of limbs and other non-mineralized tissues is rare (Zhang et al., 2012), it is geographically widespread, and such specimens are known from Sweden, Australia, England, China, and Poland (e.g., Müller, 1979; Walossek et al., 1993; Siveter et al., 2001; Zhang and Pratt 2012; Olempska et al., 2019). These exceptionally preserved fossils are invaluable for deciphering the biological relationships between individual taxa and in the broader analysis of the phylogenetic position of Phosphatocopida (Müller, 1964; Maas et al., 2003; Siveter et al., 2003; Olempska et al., 2019 for a recent summary). Phosphatocopids have long been associated with phosphate-rich pyritic limestone and black shale sedimentary deposits, many of which signal low oxygen in the marine environment (Williams et al., 2011; Supplementary Data 1), and this group may therefore be useful paleobiological indicators of environmental

Here we describe a new phosphatocopid genus and species from the first exceptionally preserved specimen found in the Cambrian of the USA, *Planamandibulus nevadensis* n. gen n. sp. Its occurrence in late Cambrian (Furongian, Stage 10) deposits of paleocontinental Laurentia fills a gap in the geographical record of this group. We integrate this new occurrence data with a global compilation data set of Cambrian phosphatocopids to assess their spatial and temporal distributions and to evaluate the main environmental and biogeographical controls on their distribution.

## **Materials and methods**

New material from Laurentia. We present new phosphatocopid material from petroliferous limestones in the upper Windfall Formation, Cambrian Stage 10 (from the Eoconodontus Biozone; for which, see Miller et al., 2015), from a section in Ninemile Canyon, Antelope Range, Nevada. These fossils were recovered during analysis of rock for conodonts by heavy-liquid and magnetic separation following 10% acetic acid treatment. Several individual phosphatocopids were recovered, most of which are indeterminate carapaces, but one preserves internal anatomy. Specimen was mounted on a 3 mm brass stub using clear nail varnish and volumetrically characterized using synchrotron radiation X-ray tomographic microscopy (SRXTM). Measurements were taken using ×10 objective lenses at 14 keV. For each data set, 1,501 projections over 180° were acquired, resulting in volumetric data with voxel sizes of 0.65 µm. These experiments were performed on the TOMCAT beamline at the Swiss Light Source, Paul Scherrer Institut, Villigen, Switzerland. The resultant ~1,250 images were rendered into a threedimensional volume using the imaging software Dragonfly and Avizo, from which anatomy was then determined by identifying and highlighting the structures on each image. The new material from the upper Windfall Formation is among the youngest occurrences of phosphatocopids from the Cambrian (Fig. 1).

*Phosphatocopid occurrence data.* We have compiled our phosphatocopid occurrence data set on the basis of a primary review of

literature from which 101 occurrences comprising 75 phosphatocopid taxa, including 26 genera and several taxa listed in open nomenclature, are examined (Fig. 1; Supplementary Data 1). Our data set includes phosphatocopid material from North America (United States, Canada), Europe (United Kingdom, Scandinavia, Poland, glacial erratics from Germany), central Asia (Kazakhstan, Kyrgyzstan), China, Australia, and Antarctica (glacial erratics from King George Island). We note that there are large geographical gaps in the fossil record of phosphatocopids. In particular, there are no specimens reported from South America, Africa, or south and southeast Asia, which we consider to partly reflect societally influenced collection biases (Raja et al., 2022) together with the distribution of strata that typically bear phosphatocopids (especially phosphatic limestones and black shales) in Cambrian stages 3 to 10 (e.g., Cook and Shergold, 1984; Fig. 1).

Although many taxa are crudely identifiable from their carapace morphology, soft anatomy is crucial for confident taxonomy of phosphatocopids because of the problems of homoplasy with arthropod carapaces (see for example, Zhai et al., 2019). We have therefore not included some groups of putative phosphatocopids (see Maas et al., 2003) for which there are no specimens reported with nonmineralized tissues or interdorsum preserved. We have excluded the following genera from our analysis, several of which have been alternatively assigned to the polyphyletic group Bradoriida (see Williams et al., 2007): Liangshanella, Dielymella, Alutella, Flemingopsis, Gladioscutum, Oepikaluta, Pejonesia, Zepaera, Epactridion, and Monasterium. We also note that many Dabashanella species names are synonyms (see Hou et al., 2001) and have accounted for this in our data compilation (Supplementary Data 1).

In our compilation of data, we noted uncertainties in the definition of some taxa at the family level (see Maas et al., 2003) and use genera rather than families to interrogate paleodistribution patterns. We note that some authors regard the genus *Hesslandona* as polyphyletic (e.g., Zhang and Dong, 2009), and we thus identify a core *Hesslandona necopina* Müller, 1964 group, which includes that type species and *H. curvispina* Maas et al., 2003, *H. ventrospinata* Gründel in Gründel and Buchholz, 1981, *H. trituberculata* Lochman and Hu, 1960, Rushton, 1978, *H. longispinosa* (Kozur, 1974) sensu Zhang et al., 2011, *H. toreborgensis* Maas et al., 2003, *H. suecica* Maas et al., 2003, and *H. kinnekullensis* Müller, 1964 (see Zhang et al., 2011), and a broader group, *Hesslandona* sensu lato, which also includes *H. unisulcata* Müller, 1982 and *H. angustata* Maas et al., 2003.

Quantitative analyses. We analyzed the temporal and spatial patterns of phosphatocopid occurrences in our data set to evaluate the underlying controls on their occurrence in the fossil record. Quantitative analyses were conducted in the statistical software package R (R Core Team, 2021). Present-day coordinates of occurrences were rotated to their midpoint age paleopositions using the "reconstruct" function of the "rgplates" package (Müller et al., 2018; Kocsis et al., 2024). Of the 94 occurrences with known present-day coordinates, all were paleorotated on the Merdith et al. (2021) rotation model, all but two occurrences were paleorotated on the PALEOMAP rotation model (Scotese and Wright, 2018), and all but three (including Planamandibulus) were paleorotated on the Torsvik and Cocks (2016) rotation model (see Supplementary Data 1). For paleorotation, the present-day coordinates of the King George Island (Antarctica) occurrence were shifted to the Transantarctic Mountains, which is likely where the glacial erratic originated from (Wrona, 2009).

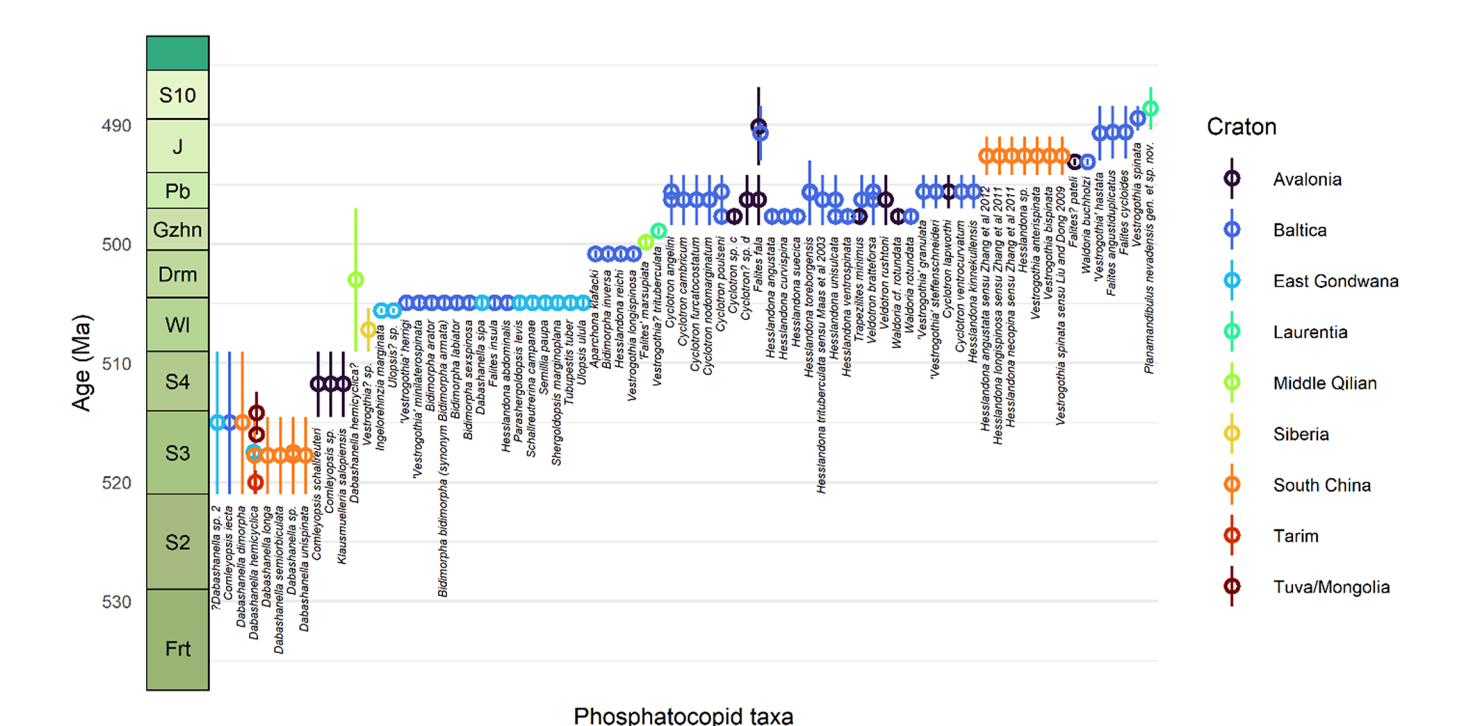


Figure 1. Phosphatocopid occurrences through the Cambrian. The majority of occurrences are from the Miaolingian and Furongian series, with particular concentrations at the Wuliuan–Drumian boundary (Baltica and East Gondwana) and throughout the Guzhangian and Paibian stages (across Avalonia, Baltica, East Gondwana, Laurentia, North China, and South China). There are no occurrences below Stage 3 and a paucity of occurrences in the upper Cambrian, above the Paibian Stage. Circles represent occurrence best-estimate ages; vertical lines represent occurrence age uncertainties; colors represent the craton (paleocontinent) of each occurrence. For details of stratigraphy and age assignments, see Supplementary Data 1. Timescale produced using the 'deeptime' package (Gearty, 2024). The phosphatocopid-bearing level in the upper part of the Bitao Formation at the Wangcun Section, western Hunan, is reported to be from strata assignable to the Westergaardodina of. W. calix—Prooneotodus rotundatus Zone by Zhang et al. (2011, 2012) and Zhang and Dong (2009). Those authors referred this level to the Paibian Stage. Bagnoli et al. (2014) correlated the Westergaardodina of. W. calix—Prooneotodus rotundatus Zone with the Westergaardodina aff. W. fossa—Prooneotodus rotundatus Zone of North China, which is above the Paibian Stage, and Dong and Zhang (2017) record this level as Jiangshanian. Accordingly, for the purpose of this paper, we have referred the taxa from the Wangcun Section, including those given by Dong et al. (2005), Zhang and Dong (2009), and Zhang et al. (2011, 2012), including Hesslandona necopina, H. longispinosa, H. angustata, Vestrogothia anterispinata Zhang and Dong, 2009, V. bispinata Zhang and Dong, 2009, and V. spinata Müller, 1964, to the Jiangshanian, while noting that there is some uncertainty in this assignment, and they may be Paibian.

Numerical model simulations. Climate model simulations were performed using the HadCM3L general circulation model (GCM) by the BRIDGE group at the University of Bristol; it has been widely applied in deep-time paleoclimate studies. The simulations used here are from the "tfks" series of simulations, with pCO<sub>2</sub> values tuned to match the global mean surface temperatures of Scotese et al. (2021), and are the same as the "scotese\_08" simulations of Judd et al. (2024). The "tfks" simulations are archived in the Providing Unified Model Access (PUMA) code archive.

Assessment of paleoenvironment. We have estimated water-column oxygen level and water depth from data in the original publications (Supplementary Data 1). We have used the presence of pyrite, phosphorites, glauconite, olenid trilobites, high organic content, petroliferous facies, "stinkstones" (sulfur-rich), and black shales—sometimes in combination—as indicators of low oxygen level in the Cambrian water column. We used reported sedimentary criteria to assess whether deposits formed at or above storm wave base as a means of differentiating between more nearshore shallow marine settings and more offshore deeper settings (i.e., below storm-wave base would be a minimum several 10s of meters depth).

Repositories and institutional abbreviations. Specimens and additional data examined in this study are deposited in the following institutions: Oxford University Museum of Natural History (OUMNH), Oxford, UK, and University of Plymouth PURE repository, Plymouth, UK.

## Systematic paleontology

Phylum **Euarthropoda** Lankester, 1904 Class **Pancrustacea** Zrzavý and Štys, 1997 Order **Phosphatocopida** Müller, 1964 Family **Cyclotronidae** Gründel and Buchholz, 1981 Genus **Planamandibulus** new genus

Type species. By monotypy, Planamandibulus nevadensis new species.

*Diagnosis.* Cyclotronid with uniramous antenna (a2) in combination with a mandible (a3) that bears an endopod with three podomeres and a large plate-like exopod.

*Etymology. Plana*, Latin for flat, and *mandibula*, the third appendage of phosphatocopids. This name alludes to the plate-like shape of the exopod (a3) that is unique to the holotype and is one of the distinguishing features that separate this genus from other Phosphatocopida (notably from its closest relative, *Cyclotron*).

*Remarks.* A uniramous antenna (a2) is shared only with *Cyclotron* Rushton, 1969 (see Olempska et al., 2019, fig. 2a), whereas in all other phosphatocopids, this limb is biramous. However, in *Cyclotron*, the mandible (a3) is distinctly different from that of *Planamandibulus*, with a two-podomere-bearing endopod and a small exopod (Olempska et al., 2019, fig. 2b). The post-mandibular limbs

of *Planamandibulus* are very similar to those of *Cyclotron*: compare limbs a4 and a5 (Fig. 3.3, 3.4) with Olempska et al. (2019) figure 2c, and limbs a6 and a7 (Fig. 3.5, 3.6) with Olempska et al. (2019) figure 2d.

# **Planamandibulus nevadensis** new species Figures 2, 3

*Holotype.* OUMNH PAL-AT.00740, a carapace with preserved appendages, from a sample of dark gray, petroliferous carbonate concretions within fine-grained laminated carbonate in the upper Windfall Formation, Furongian (Stage 10), from a section in Ninemile Canyon, Antelope Range, Nevada (39.20°N, 116.26°W). The sample yields hundreds of pristinely preserved conodonts of the *Eoconodontus* Biozone.

*Diagnosis.* Valves sub-elliptical bearing a low-relief subcircular anterodorsal node and a low-relief but more elongate posterodorsal lobe. Uniramous antenna (a2) in combination with a mandible (a3) that bears an endopod with three podomeres and a large plate-like exopod. Well-developed and large bifurcate caudal process at posterior termination of body.

#### Description

Carapace. Valves sub-elliptical in lateral view (Fig. 2.1, 2.2), ~1.2 mm long. Lobation as in diagnosis. Valve margin weakly flattened, without marginal rim.

Antennule (a1). The antennules are not preserved.

Antenna (a2). The second appendage is uniramous. The proximal part of the limb branch, presumed to be a syncoxa (coxa + basipod), is wedge-shaped, bends medially and broadens distally, and is ~250  $\mu$ m long (Fig. 3.1). The endopod arises laterodistally from the proximal limb branch. Its differentiation into discrete podomeres cannot be discerned, but it possesses ~12 setae, which fan out from its perimeter. The endopod is flattened slightly and is ~100  $\mu$ m long (Fig. 3.1, en, sa).

Mandible (a3). The third appendage is biramous and ~300  $\,\mu m$  long (not including endopodal spines). The proximal limb branch (presumed coxa and basipod, although differentiation between the two is unclear) is ~180  $\,\mu m$  long and bears several setae toward its distal inner end (Fig. 3.2, plb, sa). The endopod has three podomeres, which narrow distally: podomeres one and three bear eight setae on their inner enditic surface, and podomere two bears four with no evidence of an enditic surface. A long, sub-ovate and plate-like exopod arises mesiodistally from the proximal limb branch and is fringed by at least 21 setae (Fig. 3.2, ex, sa).

First and second post-mandibular limbs (a4 and a5). The fourth appendage is biramous and  $\sim\!300~\mu m$  long (not including setae). Its proximal limb branch is  $\sim\!150~\mu m$  long and comprises basipod and proximal endite (Fig. 3.3, 3.4). The basipod is sub-triangular in overall shape,  $\sim\!100~\mu m$  long, and bears about 12 setae. The proximal endite bears about 17 setae. The endopod is  $\sim\!100~\mu m$  long and bears two podomeres. The proximal podomere has a medial endite from which seven setae arise (Fig. 3.3, en, pdm). The distal podomere is slightly narrower, has a rounded and tapering end, and bears six setae. The exopod is  $\sim\!150~\mu m$  long, paddle-shaped, does not taper distally, and at its margin bears at least 19 setae. The second post-mandibular limb (a5) displays similar morphology.

Third and fourth post-mandibular limbs (a6 and a7). The sixth and seventh appendages are biramous and ~250  $\,\mu m$  long (not including setae). They comprise a broad, sub-rectangular basipod that does not bear setae and accounts for just under half the length

of the appendage (Fig. 3.5, 3.6). The exopod is leaf-shaped, narrows distally, and is fringed by about 19 setae (Fig. 3.5, 3.6, ex, sa). The endopod, although not always visible, is evident on a7 as a structure that tapers distally and appears to be fringed by up to 7 setae medially (Fig. 3.6, en).

Terminal end of body. The terminal segment of the body is developed into two lateral bulges, behind which is a large bipartite caudal process ~450  $\mu m$  long (Fig, 3.73.9). Each branch bears a row of 10 spines that are directed posteroventrally along the medial and exterior surfaces and appear to correlate to segments in each branch. The spines are ~75  $\mu m$  long. The base of the structure has a medial groove terminating before the two branches. At the base of the two branches are two distally pointing bulges.

Additional morphological features. Adjacent to the antenna (a2) and near the front of the animal are the remnants of soft anatomy (Fig. 2.5). Remnants of the trunk, perhaps  $\sim 800~\mu mlong$ , are also preserved (Fig. 2.7, 2.8).

Etymology. Nevadensis is Latin for Nevada, in reference to the mountain range and state of Nevada where the holotype was discovered.

*Material.* Only the holotype. Several indeterminate phosphatocopid carapaces are associated with this.

Remarks. Planamandibulus nevadensis n. gen. n. sp. is ~1.2 mm long and compared with carapaces of Cyclotron lapworthi Groom 1902, Rushton, 1969, which reach 5 mm long in adults (Williams et al., 1994), is probably a juvenile instar. Planamandibulus nevadensis co-occurs with several other indeterminate phosphatocopids in deposits that represent grain flow in a mid- or upper-slope regime and in a dysoxic or an anoxic setting (Cook and Taylor, 1977; Taylor and Cook, 1977). The phosphatocopids may have been transported downslope in the grain flows. However, the fully articulated soft anatomy of P. nevadensis suggests minimal transport. Associated taxa include the agnostoid *Lotagnostus*, the olenid trilobite Bienvillia sp., and a fragmentary pygidium of Hedinaspis sp. The agnostoids and trilobites were disarticulated and probably transported before deposition. Repetski et al. (2019) confirmed that Lotagnostus is abundant in deep basinal marine facies but nearly absent from shallower marine deposits (Westrop et al., 2011; Tortello, 2014). This restricted distribution supports Landing and Westrop (2015), who noted Lotagnostus occurs together with phosphatocopids in dysoxic settings and is a pattern we examine in more detail in the following sections.

#### **Discussion**

Temporal and lithofacies distribution of phosphatocopid occurrences. The majority of phosphatocopid occurrences are from the Miaolingian and Furongian series, with particular concentrations around the Wuliuan–Drumian boundary and the Guzhangian and Paibian stages (Figs. 1, 4). The oldest known phosphatocopid occurrences are from Cambrian Stage 3 deposits (maximum age of ca. 521 Ma) of South China, Baltica, and East Gondwana (Fig. 1; e.g., Zhang and Pratt, 2012). The youngest known phosphatocopids are those newly reported here from Laurentian deposits (from the Eoconodontus Biozone; see Miller et al., 2015) that are about 489 Ma, along with taxa from Avalonian and Baltic deposits. The greatest species and genus diversity occurs in the upper Guzhangian to lower Paibian interval (Fig. 1), and similar numbers of taxa are also known from the uppermost Wuliuan Stage. However, there are

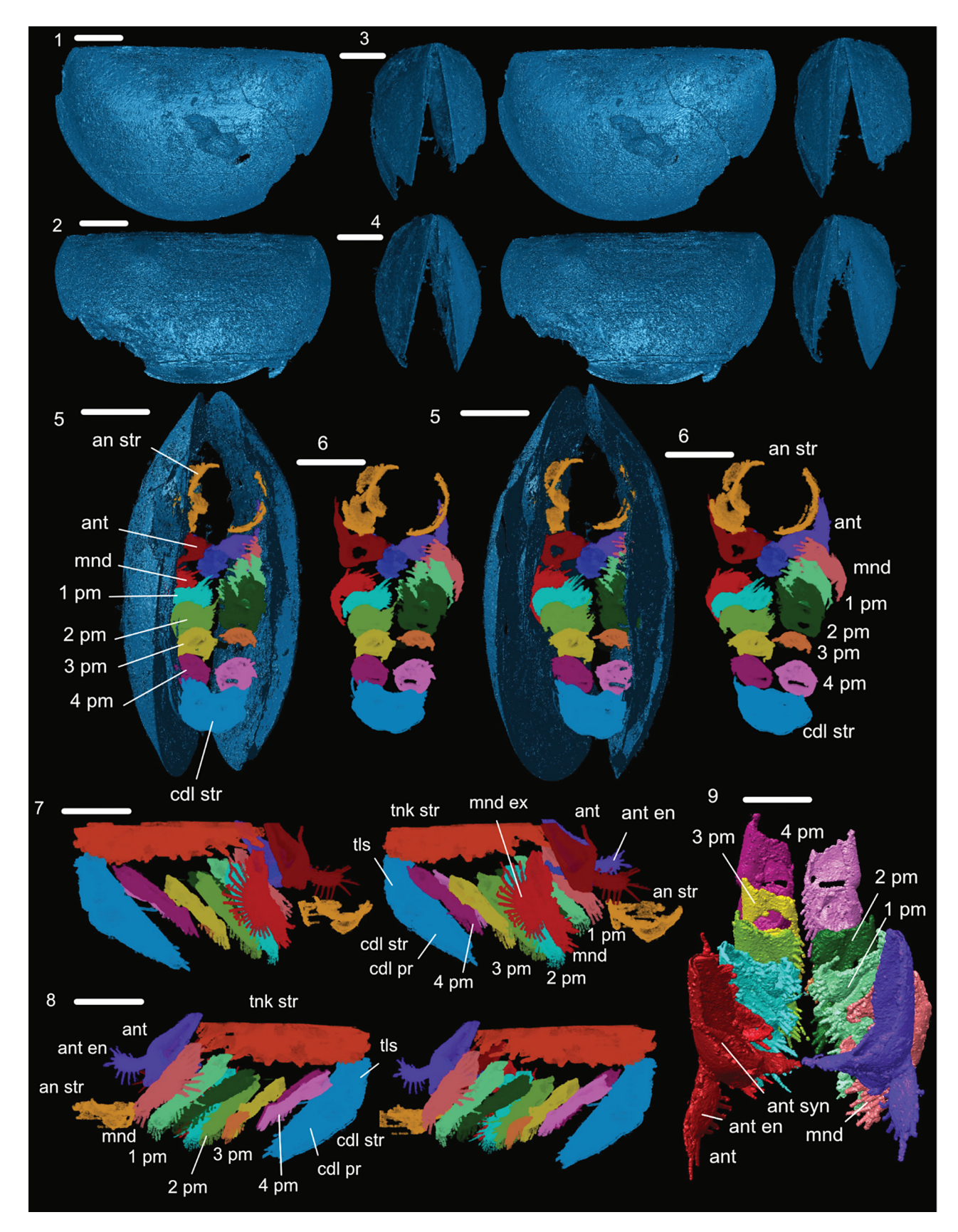


Figure 2. Holotype of *Planamandibulus nevadensis* n. gen. n. sp., virtual reconstructions of carapace with soft parts. (1) External right lateral view, posterior to anterior (stereo pair). (2) External left lateral view, anterior to posterior (stereo pair). (3) External anterior view of valves (stereo pair). (4) External posterior view of valves (stereo pair). (5) Ventral view (stereo pair). (7) Right lateral view, posterior to anterior with valves removed (stereo pair). (8) Left lateral view, anterior to posterior with valves removed (stereo pair). (9) Medial anterior to posterior view of appendages 2–7 with valves removed. Scale bars = 100 μm. an str = anterior structure; ant = antenna (a2); ant en = antenna (a2) endopod; ant syn = antenna (a2) syncoxa; mnd = mandible; mnd ex = mandible exopod; 1 pm = first post-mandibular limb; 2 pm = second post-mandibular limb; 3 pm = third post-mandibular limb; 4 pm = fourth post-mandibular limb; cdl str = caudal structure; tls = telson; cdl pr = caudal process; tnk str = trunk structure.

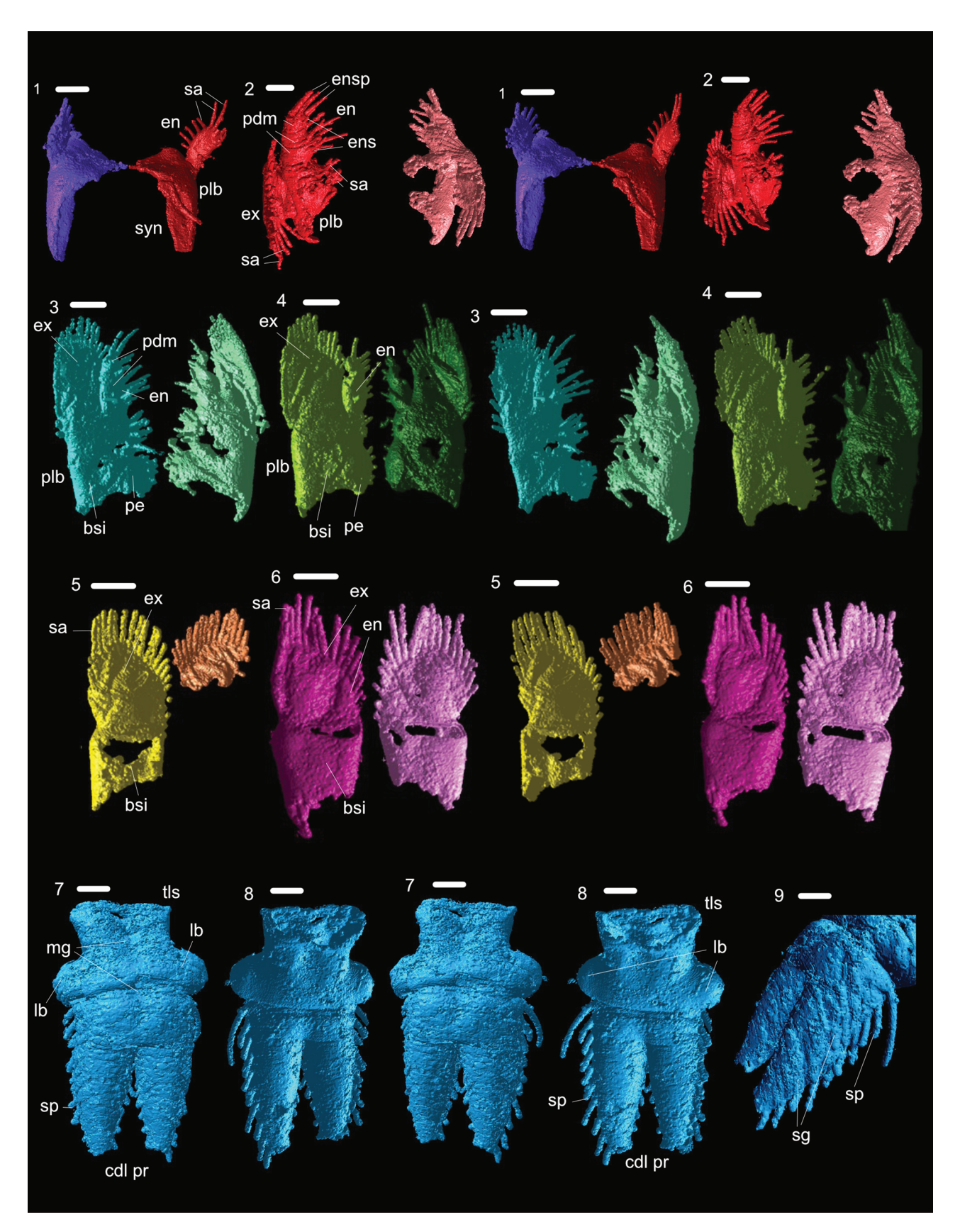


Figure 3. Soft anatomy of *Planamandibulus nevadensis* n. gen. n. sp., virtual reconstructions of individual limbs. (1) Dorsal-anterior view of antenna (a2) (stereo pair). (2) Inverted anterior view of mandibles (stereo pair). (3) Inverted posterior view of first post-mandibular limbs (stereo pair). (4) Inverted posterior view of second post-mandibular limbs (stereo pair). (5) Inverted posterior view of third post-mandibular limbs (stereo pair). (6) Inverted posterior view of fourth post-mandibular limbs (stereo pair). (7) Posterior view of caudal structure (stereo pair). (8) Anterior view of caudal structure (stereo pair). (9) Right ventral-lateral view of caudal process on caudal structure. Scale bars = 50 μm. en = endopod; syn = syncoxa; plb = proximal limb branch; sa = setae; ensp = endopodal spines; ens = endtitic surface; ex = exopod; bsi = basipod; pdm = podomeres; pe = proximal endite; tls = telson; cdl pr = caudal process; mg = medial groove; lb = lateral bulge; sp = spine; sg = segment.

too few occurrences (and taxa) to draw any robust conclusions about phosphatocopid diversity through time. The Wuliuan–Drumian boundary concentration of occurrences are all from Baltica (Borregard Member, Bornholm, Denmark) and East Gondwana (Arthur Creek and Beetle Creek formations, northern Australia). The Guzhangian–Paibian concentration of occurrences are predominantly from Avalonia (United Kingdom and eastern Canada) and Baltica (Sweden, Germany, and Poland), with additional specimens from North China (China) and Laurentia (United States) confined to the lower Guzhangian. Additional occurrences are known from Jiangshanian to Stage 10 deposits of South China (China), Avalonia (United Kingdom and eastern Canada), Baltica (Sweden and Germany), and Laurentia (United States).

The temporal occurrence and abundance of phosphatocopids correspond to particular lithofacies (Supplementary Data 1), notably black shale horizons that are sometimes associated with pyritiferous limestones (stinkstones), phosphatic or glauconitic limestones, and phosphorites. This lithofacies control limits the utility of phosphatocopids for biostratigraphical analysis, although a few taxa that are closely associated with certain trilobite zones, such as the Paibian *Cyclotron lapworthi*, have interregional correlative value (Williams et al., 1994; Williams and Siveter, 1998).

In the Anglo-Welsh Cambrian succession, which has been collected for over 100 years, phosphatocopids occur only in the glauconite- and pyrite-rich Comley Limestones of Stage 4 (lower Comley Group) and the black shale facies that characterize the upper Miaolingian and lower Furongian (e.g., Outwoods Shales Formation) on the Midland Craton (Williams and Siveter, 1998). Phosphatocopids are essentially absent from the less organic-rich mainly sandstone, mudstone, and turbidite deposits of the early Paleozoic Welsh Basin and the adjacent shelf (e.g., of the upper Comley Group). In the Baltic region (Scandinavia, Poland), phosphatocopid occurrences are associated with the glauconitic and pyritic limestones (Borregard Member/Exsulans Limestone), black shales, and stinkstones of the Miaolingian and Furongian Alum Shale Formation (Maas et al., 2003) but are absent from less organic-rich siliciclastic deposits of the Terreneuvian and Series 2 (Calner et al., 2013).

In South China, phosphatocopid occurrences similarly correlate with black shale facies of the Series 2 (Nangaoan) Shuijingtuo Formation or are associated with exceptional preservation as phosphatized specimens in the Furongian Bitao Formation. In East Gondwana (Australia), phosphatocopids are recorded from black shales (e.g., Arthur Creek Formation) and phosphorite deposits (Beetle Creek Formation) of the Miaolingian. A few phosphatocopid taxa, notably the paleogeographically widespread *Dabashanella hemicyclica* Huo et al., 1983, occur in both phosphorite and black shales settings (e.g., Tarim, South China) and carbonates (e.g., Ajax and Mernmerna formations, Australia; Tuva/Mongolia; Supplementary Data 1).

Geographic and bathymetric distribution of phosphatocopids. There are two predominant spatial patterns in our phosphatocopid database: paleobiogeographic and paleobathymetric. At the genus level, most taxa are found at either low (approximately <30°) or mid-to high (approximately >45°) paleolatitudes, excepting Hesslandona and Vestrogothia, which span low to mid-paleolatitudes. There is a temporal trend throughout the Cambrian from a lower paleolatitude dominance in Stage 3 and the Wuliuan Stage toward a mid-to high paleolatitude dominance from the Guzhangian onward (Figs. 4, 5). These results are robust to the choice of plate rotation model.

Most genera also occur preferentially in either shallower or deeper water settings. However, although many genera are known exclusively from shallow-water deposits, the deeperwater-occurring genera are often also known from a smaller number of shallow to mid-depth deposits (e.g., *Dabashanella*, *Hesslandona*). There is a temporal trend in the water-depth preferences of occurrences through the Cambrian, with more shallower water occurrences before the Drumian and more deeper water occurrences from the Guzhangian onward (Fig. 5). Note, however, that there are a large number of deeper water occurrences in Stage 3 deposits as well (Fig. 5), driven by *Dabashanella* occurrences in South China.

Phosphatocopids are known from a range of depositional settings, including shallow marine carbonates and phosphorites, as well as outer shelf settings characterized by black shales and pyritic limestones. Phosphatocopids commonly, although not exclusively, occur in facies indicative of low environmental oxygen levels (Supplementary Data 1). Across the data set, 60% of occurrences are from likely low-oxygen settings, and only 15% of occurrences are from settings that are unlikely to be characterized as low oxygen (the remaining 25% are "unknown" or "possibly" low oxygen; Fig. 6; Supplementary Data 1). From the Drumian through Paibian stages, the proportion of occurrences from likely low-oxygen settings is between 69 and 80%, with the absolute number of likely low-oxygen-setting occurrences peaking during the Paibian Stage (18 of 24 occurrences; Fig. 6).

The earliest phosphatocopid assemblages, within stratigraphic uncertainty, are from the Cambrian Epoch 2 Age 3 Yurtus Formation of Tarim (Zhang et al., 2020) and the Shuijingtuo and Heilinpu formations (Hubei and Yunnan provinces) of the South China paleoplate (Hou et al., 2001) and include several species of Dabashanella in deep shelf settings. One of these taxa, Dabashanella hemicyclica, is paleogeographically widespread and also occurs in shallow to mid-shelf carbonates of the approximately contemporaneous Besh-Tash and Shabakta formations of the Tuva/Mongolia terrane (Malyi Karatau and Talas Alatau terranes) of central Asia (Melnikova et al., 1997) and the shallow shelf carbonates of the Ajax and Mernmerna formations of East Gondwana (Australia; Topper et al., 2011). Other taxa of Epoch 2 include the Avalonian Comleyopsis schallreuteri Hinz-Schallreuter, 1993 and Klausmuelleria salopiensis Siveter et al., 2003 in the shelf marine carbonates of the Lower Comley Limestones, Welsh Borderland of the United Kingdom (Cambrian Age 3 to Age 4; Siveter et al., 2003).

A further group of phosphatocopids occur in shallow marine phosphorite depositional settings of the early Miaolingian (Wuliuan) in East Gondwana (Australia). These include the assemblages from the Monastery Creek Phosphorite Member of the Beetle Creek Formation in Queensland, Australia (Valetich et al., 2022), which includes endemic species of *Parashergoldopsis*, *Schallreuterina*, *Semilia*, *Dabashanella*, and *Tubupestis*, and *Ulopsis* and *Ingelorehinzia* from the Arthur's Creek Formation of the Northern Territories (Jones and Laurie, 2006; Jones and Kruse, 2009).

Late Miaolingian (Guzhangian) and early Furongian (Paibian) phosphatocopids typically occur in pyritic black mudstones and interbedded nodular limestones and mudstones that were deposited in deep, outer shelf settings (Fig. 6). Associated minerals include glauconite and phosphate (Supplementary Data 1) and, together with pyrite and high-organic-matter content of the deposits (sometimes referred to as petroliferous), point toward low-oxygen seabed conditions at the time of deposition. This is the context for most of the taxa from Baltica and Avalonia, which are found predominantly in the black shales of the Outwoods Shales

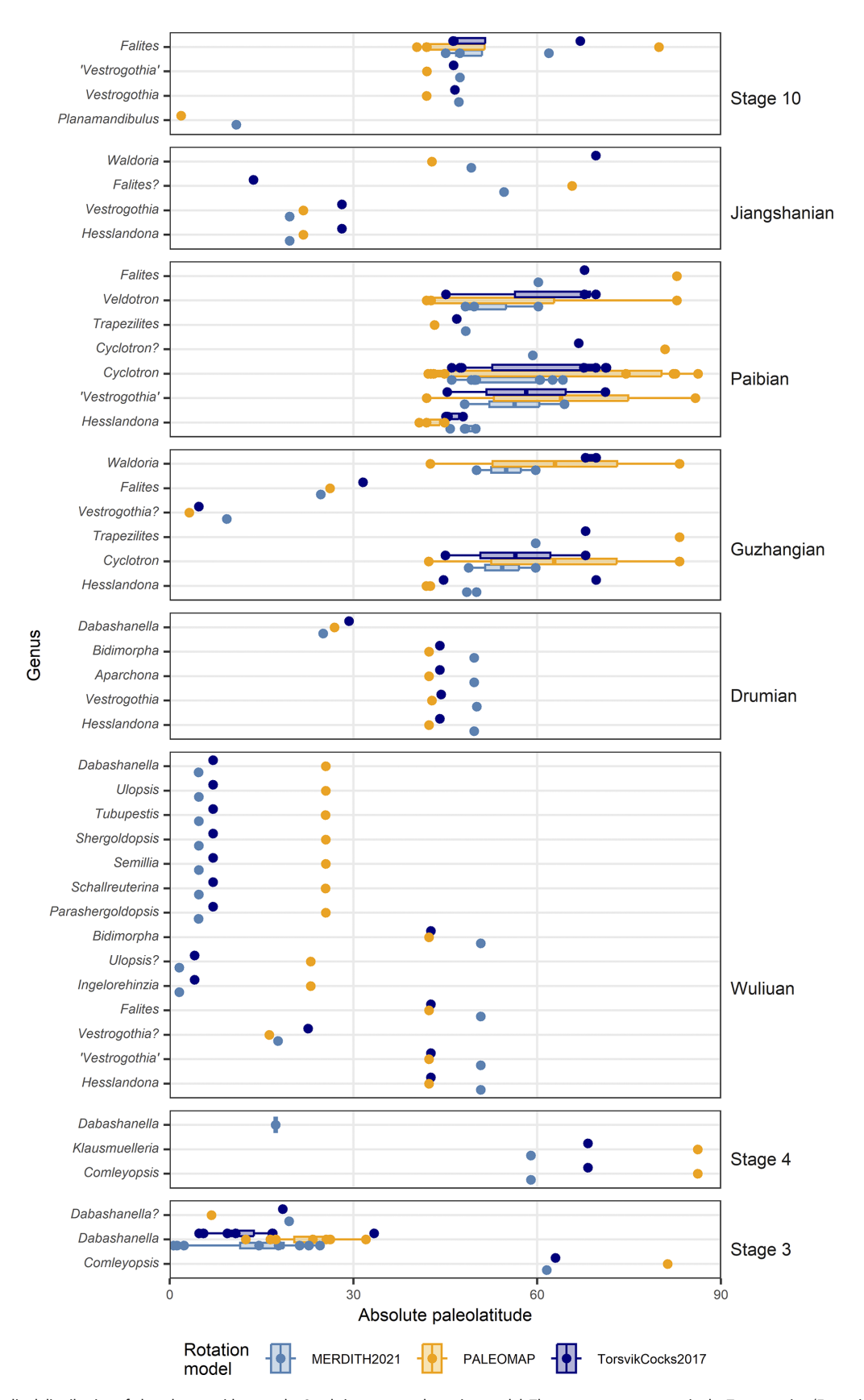


Figure 4. Paleolatitudinal distribution of phosphatocopid genera by Cambrian stage and rotation model. There are no occurrences in the Terreneuvian (Fortunian Stage and Stage 2). Series 2 (stages 3 and 4) occurrences are sparse but span low, middle, and high paleolatitudes. Lower and middle Miaolingian (Wuliuan and Drumian stages) occurrences are sparse, but not from high paleolatitudes. Upper Miaolingian through middle Furongian (Guzhangian to Jiangshanian) occurrences are more commonly high paleolatitude, and notably so during the Paibian Stage. Sparse Stage 10 occurrences include low to high paleolatitude taxa. Colors represent different continental configurations (rotation models): light blue = MERDITH2021 (Merdith et al., 2021); orange = PALEOMAP (Scotese and Wright, 2018); dark blue = TorsvikCocks2017 (Torsvik and Cocks, 2016).

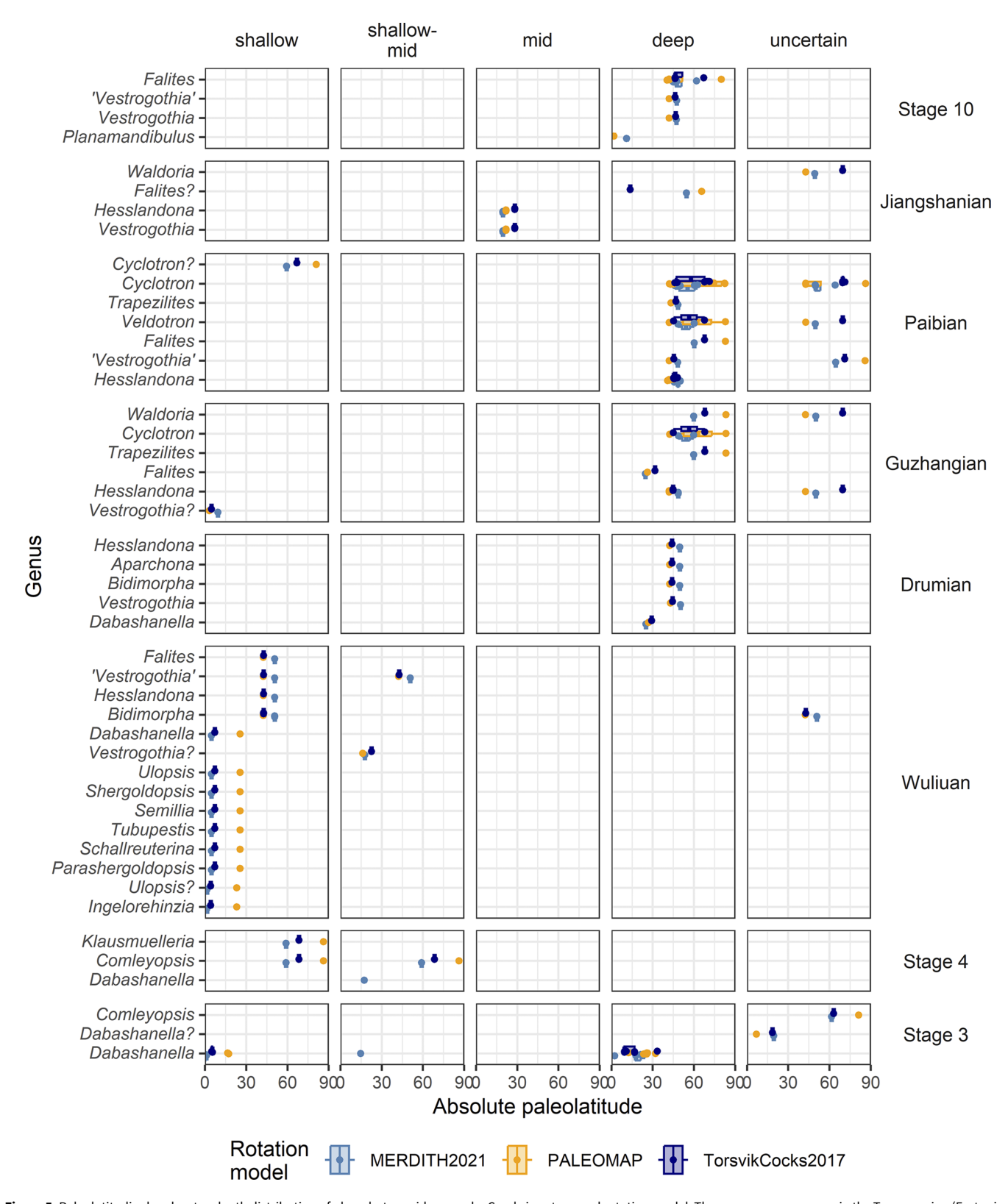
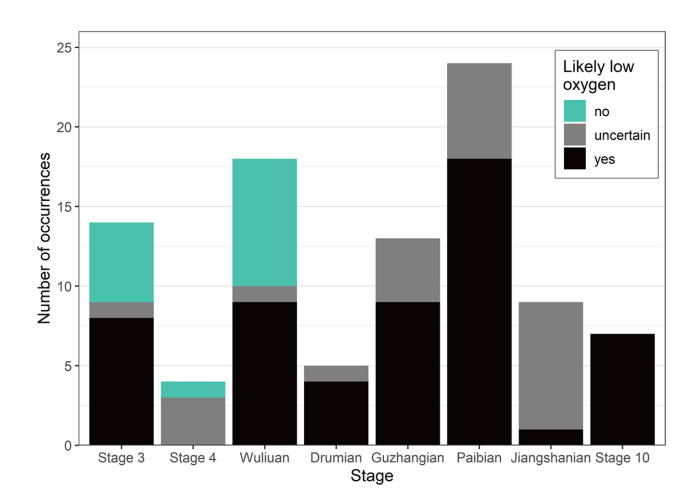


Figure 5. Paleolatitudinal and water-depth distribution of phosphatocopid genera by Cambrian stage and rotation model. There are no occurrences in the Terreneuvian (Fortunian and Stage 2). There is a shift from lower paleolatitudinal distributions during Series 2 to the Wuliuan Stage to a higher paleolatitudinal preference in the Drumian through Jiangshanian stages. The Stage 10 occurrences are low and high paleolatitudes. There is a concomitant shift in water-depth preference from mixed or shallower preference until the Wuliuan, to deeper preference from the Drumian onward. Colors represent different continental configurations (rotation models): light blue = MERDITH2021 (Merdith et al., 2021); orange = PALEOMAP (Scotese and Wright, 2018); dark blue = TorsvikCocks2017 (Torsvik and Cocks, 2016).



**Figure 6.** Number of occurrences by Cambrian stage and their identified marine oxygenation conditions based on the geological setting of each occurrence. The majority (50%) of phosphatocopid occurrences are from likely low-oxygen settings, with only 15% of occurrences from settings identified as not likely to have a low oxygen concentration; the remaining 35% of occurrences are from settings where we are uncertain of the oxygenation state. From the Drumian onward, all occurrences are from either uncertain or low oxygen settings.

Formation in Warwickshire, England (Williams and Siveter, 1998), and "stinkstones" and mudstones of the Alum Shales Formation of southern Sweden (e.g., Maas et al., 2003). Associated taxa include olenid trilobites that are thought to signal low-oxygen conditions (e.g., Fortey, 2000, 2014). Phosphatocopid taxa that are exclusive to such facies include *Aparchona*, *Bidimorpha*, *Waldoria*, *Veldotron*, *Trapezilites*, *Cyclotron*, and *Falites* species and the majority of *Hesslandona* (*neocopina* and broader groups) and *Vestrogothia* species (Supplementary Data 1). The late Furongian *Planamandibulus nevadensis* n. gen n. sp. is also associated with dysoxic sedimentary facies in the upper Windfall Formation of Nevada, USA. During the late Miaolingian and Furongian, phosphatocopids are only very rarely reported from more inshore and shallower water facies (Fig. 5; Supplementary Data 1).

Latitude and sea temperature controls on phosphatocopid distribution. The lithofacies distribution patterns of phosphatocopids suggest an association with low-oxygen environments, but the group also demonstrates clear paleolatitudinal differentiation of taxa, and here we compare these patterns with paleoclimate model simulations of sea surface and below sea surface Cambrian ocean temperatures. We plot the latitudinal distributions of taxa according to three continental rotation models (Torsvik and Cocks, 2016; PALEOMAP: Scotese and Wright, 2018; MERDITH2021: Merdith et al., 2021). Although absolute paleolatitudes and positions vary between the different models, the overall patterns are remarkably consistent (Fig. 5). Phosphatocopid occurrence data are available for Cambrian ages 3 to 10, but it is the patterns identified in the Guzhangian (late Miaolingian) and Paibian (early Furongian) that provide the greatest detail as these have the widest geographical spread. We identify species that suggest warm-water and coolwater preferences.

In Cambrian Epoch 2 (Age 3), and later in the early Miaolingian (Wuliuan), *Dabashanella* possessed an essentially low-latitude (<35°) range and occurred in both shallow marine and deeper shelf settings (Fig. 5). Comparison with climate models for this interval suggests that shallow marine *Dabashanella* species lived in surface waters typically of about 25 to 30 °C but extended into deeper water

settings (below storm-wave base) that may have been as cool as 20 ° C. The wide geographical distribution of *Dabashanella* species between East Gondwana, South China, Tarim, and Tuva/Mongolia, but their absence from higher paleolatitude sites, suggests this was a warm-water taxon. By comparison, the late Epoch 2 *Comleyopsis* and *Klausmuelleria* occur at high southern paleolatitudes (>60°S) likely in water temperatures modeled to between 5 and <15 °C. We note that the single occurrence of an unidentified phosphatocopid in the lower Comley Limestones (Series 2) of the Welsh Borderland that resembles *Dabashanella* (Williams and Siveter, 1998, pl. 6, figs. 9, 10) might challenge these assumptions if further evidence is identified.

The shallow marine shelf taxa of early Miaolingian age that are endemic to East Gondwana (Australia), namely *Ulopsis, Ingelore-hinzia, Parashergoldopsis, Schallreuterina, Semilia*, and *Tubupestis* may represent a warm-water-adapted tropical phosphatocopid assemblage, likely in waters modeled to between 25 and 30 °C. None of these taxa has been reported elsewhere from eastern Gondwana or adjacent paleocontinents, but the phosphatocopid *Dabashanella*, which is also a component of these assemblages, does occur in South China, Tarim, and Tuva/Mongolia, suggesting that environmental barriers, including temperature, and not geography, were a key control on the endemic taxa.

Late Miaolingian and early Furongian phosphatocopid occurrences cover a wide paleolatitudinal range, but most faunas have been described from paleocontinental Baltica and Avalonia. These include the taxa *Aparchona*, *Bidimorpha*, *Waldoria*, *Veldotron*, *Trapezilites*, and *Cyclotron* that occur exclusively in mid- to high paleolatitude (>35 to 90°S) deep shelf sites, probably with water temperatures from 4 to 20 °C (Fig. 7). These may define a warm-temperate and temperate zone fauna, though it is notable that some of the co-occurring phosphatocopid taxa also extended into lower paleolatitudes, notably *Hesslandona* (both *necopina* and broader groups), *Vestrogothia*, and *Falites*. Although generally a mid- to high-paleolatitude taxon, *Hesslandona* is known from a mid-depth deposit low (<30°) paleolatitude deposit in the Jiangshanian, with water temperatures potentially reaching the mid-20s °C (Fig. 7).

No definitive low-paleolatitude phosphatocopid fauna is identified for the late Miaolingian and early Furongian, although rare and putative *Falites* and *Vestrogothia* are reported from the late Miaolingian of the Qilian Block (peri-South China) and Laurentia, respectively (Supplementary Data 1). Overall, this may represent a particular collection bias toward Avalonia/Baltica during this interval, and/or the absence of suitable lithofacies for phosphatocopids in other paleocontinental areas. However, the persistence of phosphatocopids in low paleolatitudes is suggested by a suite of *Hesslandona* and *Vestrogothia* species from South China in the Jiangshanian, and the late Furongian (Age 10) *Planamandibulus* n. gen., which currently is known only from low-paleolatitude Laurentia.

Oxygen levels as a control on phosphatocopid distribution. Although some of the patterns of distribution may indicate a water temperature preference, phosphatocopids have long been associated with dysoxic facies (e.g., Williams et al., 2011). This is borne out in our data set, which shows that about 60% of all occurrences are from likely low-oxygen settings, and only about 15% are unlikely to be from low-oxygen settings (the remaining ~25% are uncertain, rated "possible" low-oxygen or "unknown" settings; Fig. 6; Supplementary Data 1). From the Drumian through Paibian stages, the proportion of occurrences from likely low-oxygen settings is between 69 and 80%, with the absolute number

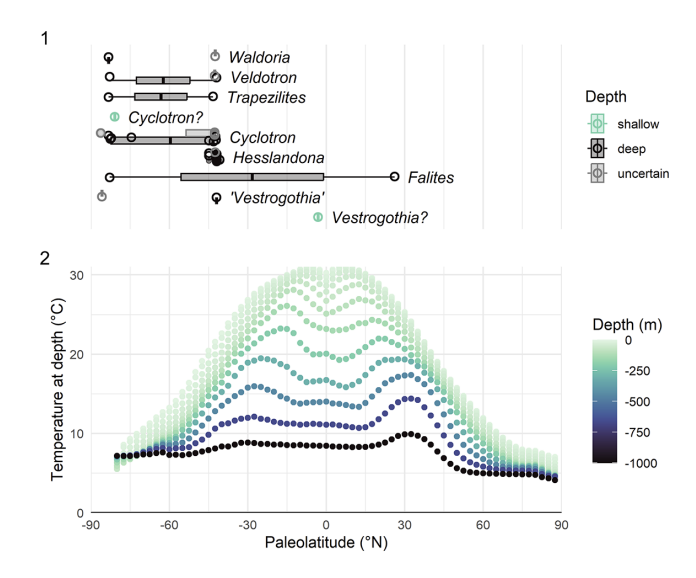


**Figure 7.** Comparison between Guzhangian + Paibian phosphatocopid occurrences (1) and modelled zonal average sea temperatures with depth (2). Note, there are no "shallow-mid" or "mid" depth occurrences for the Guzhangian or Paibian. Colors represent water depth: categorical for phosphatocopid occurrences; model ocean depth level for zonal average temperatures. Modelled sea temperatures from the HadCM3L "tfks" series 500 Ma simulation (see Judd et al., 2024, and explanation in text).

of likely low-oxygen-setting occurrences peaking during the Paibian Stage (18 of 24 occurrences; Fig. 6).

The dominant occurrence of phosphatocopids in facies that signal low ocean oxygen concentrations suggests that they may have had a capacity to recover from anaerobic shock, as demonstrated by some modern aquatic pancrustaceans (e.g., Malard and Hervant, 1999). However, it is unlikely they occupied permanently hypoxic environments as living arthropods are unable to withstand reduced oxygen for more than a few days. This resilience to low-oxygen conditions may have been present in the earliest phosphatocopids, explaining the wide geographical and environmental occurrence of *Dabashanella* in both shallower marine carbonates and deep shelf black mudstones. This environmental resilience may also explain the wide dispersal of individual species such as *Dabashanella hemicyclica* and *Hesslandona angustata* (Supplementary Data 1).

Biogeographical patterns. Biogeographical patterns have been explored in Cambrian arthropods, including trilobites and bradoriids. For trilobites, the data set is very extensive and involves some 2,460 genera from about 40 tectonostratigraphic settings worldwide (Álvaro et al., 2013). That analyzed for Bradoriida is much smaller and includes 64 genera from 20 geographical occurrences worldwide (Williams et al., 2007). By comparison, we analyze 75 phosphatocopid taxa (Fig. 1) from nine geographical regions (Fig. 8) whose reconstructed biogeographical patterns are similar to those of bradoriids and trilobites. In our analysis of biogeography, we focus on genera, mindful that higher-level taxonomy of phosphatocopids is complex, with the families Hesslandonidae, Falitidae, and Vestrogothiidae all being identified as paraphyletic and the genus Hesslandona currently ill-defined (Zhang and Dong, 2009).

For trilobites in Epoch 2, a redlichiid province has been recognized in South China and East Gondwana, an olenellid province in Laurentia, Baltica, and Siberia, and an intermediate ("overlapping") bigotinid province in peri-Gondwanan terranes (summarized by Álvaro et al., 2013). Nevertheless, phylogenetic analysis of fallotaspid trilobites within the olenellid province demonstrated close links with

redlichiid trilobites, so that a complex pattern of biogeographical relationships emerges (Lieberman, 2002). Williams et al. (2007) also recognized distinct eastern and western bradoriid assemblages for Epoch 2 and the Miaolingian, with tropical/subtropical bradoriid assemblages in East Gondwana, South China, and Siberia characterized by kunmingellids and comptalutids, and a cooler-water hipponicharionid, beyrichonid, and bradoriidid assemblage of Avalonia, Baltica, and West Gondwana. Although phosphatocopid faunas are sparsely geographically distributed through this interval, those of East Gondwana and South China are characterized by *Dabashanella* and taxa endemic to East Gondwana such as *Ingelorehinzia* and *Tubupestis*, being different from those of Avalonia and Baltica, where *Compleyopsis* and *Klausmuelleria* are reported.

Late Miaolingian and Furongian occurrences of bradoriids are too rare to define clear biogeographical regions (Williams et al., 2007), but Acado-Baltic (sometimes referred to as Atlantic) and Pacific trilobite provinces have been distinguished (patterns summarized by Álvaro et al., 2013). The Acado-Baltic province is represented by Avalonian, Baltic, certain peri-Gondwanan, and deep-water Laurentian trilobite faunas and seems to signal a coolwater setting (Álvaro et al., 2013). Late Miaolingian and early Furongian phosphatocopid faunas of Avalonia and Baltica show a pattern consistent with the Acado-Baltic province and are characterized by a cool and often deep-water assemblage of *Bidimorpha*, Veldotron, Cyclotron, Trapezilites, and Waldoria. We have noted (in the preceding) that the North American Planamandibulus n. gen. is related to *Cyclotron*, being also consistent with the extent of the Acado-Baltic trilobite province, although it may have occurred in a warmer sub-surface temperature regime. These assemblages also include Hesslandona (necopina and broader groups) and Vestrogothia, which show biogeographical links with rare phosphatocopid faunas of this age from South China, although no endemic South China or East Gondwana phosphatocopid assemblages of this age have been described.

## **Conclusions**

We describe the new phosphatocopid Planamandibulus nevadensis n. gen. n. sp. from the upper Windfall Formation (Furongian, Stage 10) of Nevada, USA. This is the first phosphatocopid from North America to be described with its soft anatomy, and it indicates an affinity with the Baltic and Avalonian genus Cyclotron. The new phosphatocopid material from Laurentia facilitates a global analysis of Cambrian phosphatocopid faunas that suggests sea temperature, seawater oxygen level, and paleogeography all exerted controls on phosphatocopid distribution. Thus, many phosphatocopids are associated with sedimentary deposits that suggest low-oxygen conditions at the seabed, vis black shales, sulfurous or petroliferous deposits, pyrite, glauconite, and associated fauna of olenid trilobites (Supplementary Data 1). These deposits become particularly widespread during the late Miaolingian and early Furongian, when records of phosphatocopids are most diverse. Patterns of paleolatitudinal differentiation identify warm-water tropical/subtropical taxa such as Dabashanella and cooler (temperate) water fauna such as Veldotron, Bidimorpha, Trapezilites, Cyclotron, and Waldoria. While some taxa exhibit wide paleogeographical connections, for example, Hesslandona (necopina and broader group) in Baltica and South China, clear biogeographical patterns emerge, with an early (Epoch 2-early Miaolingian) South China/East Gondwanan assemblage characterized by Dabashanella and ulopsids such as Tubupestis and a later (late Miaolingian-early Furongian) Avalonian/Baltic assemblage characterized

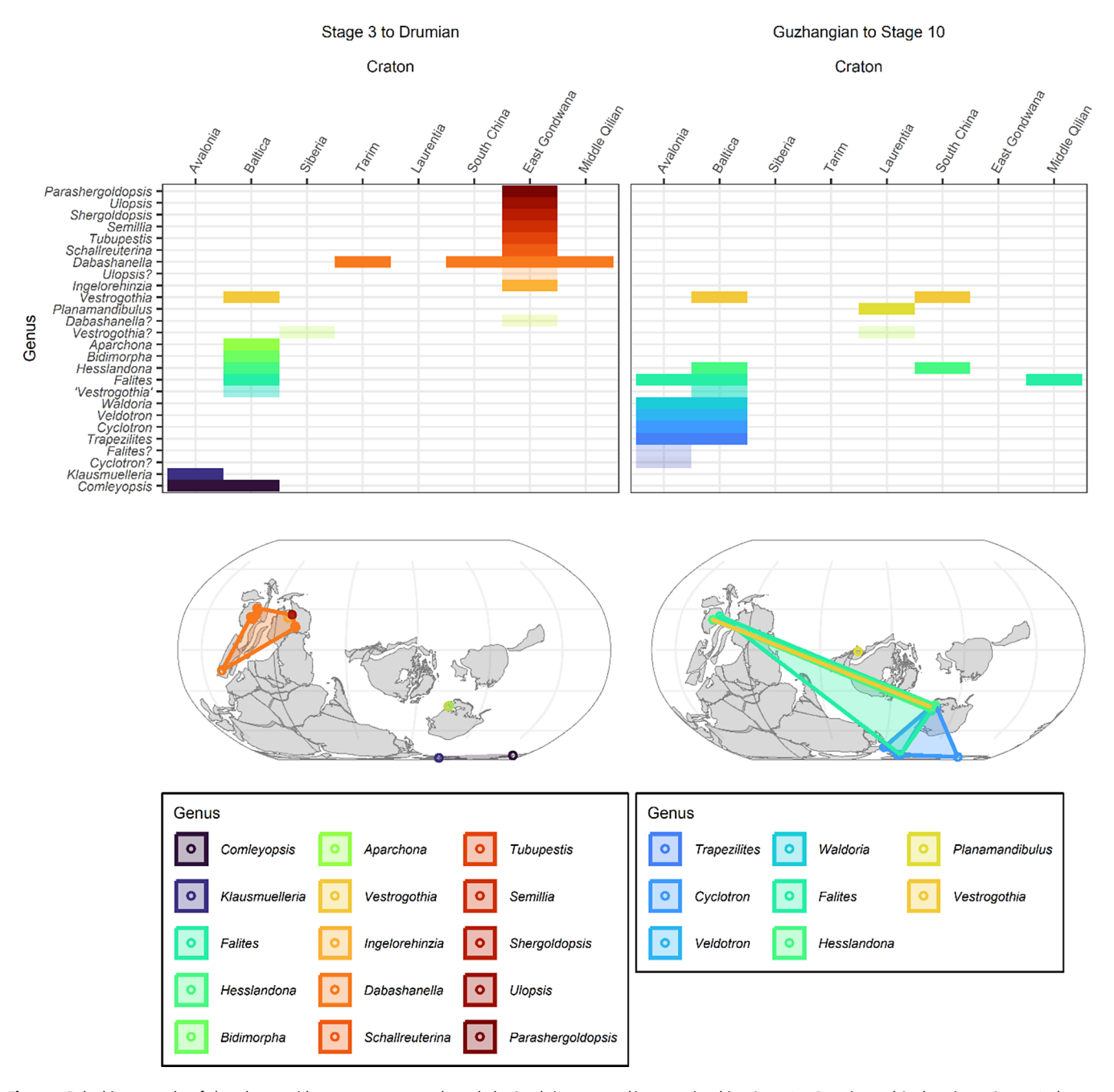


Figure 8. Paleobiogeography of phosphatocopid genera occurrences through the Cambrian, grouped into two time bins, Stage 3 to Drumian and Guzhangian to Stage 10, shown as craton presence—absence matrices and maps. For this plot only, occurrences were rotated to the midpoint ages for each set of stages (510.75 Ma and 493.675 Ma, respectively) using the PALEOMAP rotation model (Scotese and Wright, 2018). Colors represent phosphatocopid genera, including those in open nomenclature; taxa in open nomenclature are faded in the presence—absence matrices and are excluded from the paleobiogeographic maps; the color scale is consistent across all panels; convex hulls span the locations of occurrences of each genus.

by *Veldotron*, *Bidimorpha*, *Trapezilites*, *Cyclotron*, and *Waldoria*. *Planamandibulus nevadensis* from the late Furongian of the USA is the youngest phosphatocopid taxon to be described, and its depositional context in deep-water petroliferous deposits and affinities with the Baltic/Avalonian *Cyclotron* are consistent with the environmental and biogeographical patterns described here.

**Acknowledgments.** M.W., T.H.P.H., and T.W.W.H. acknowledge Leverhulme Grant RPG-2022-233 "Earth system dynamics at the dawn of the animal-rich biosphere." We also acknowledge J.F. Taylor, co-collector of the Ninemile

section, H. Belkin for assistance with initial SEM imagery, and S.W. Nixon for 3D printing. Huaqiao Z. (NIGPAS, Nanjing), D.J. Horne (Queen Mary, London), and T. Topper (Swedish Museum of Natural History) are thanked for their constructive and invaluable reviews.

## Competing interests. None.

**Data availability statement.** All data and code needed to reproduce the analyses are included in the main text and supplementary materials. The SRXTM data are available in the University of Plymouth PURE repository: https://doi.org/10.24382/5495bebb-698a-4c5f-a4ad-c7cc9367c4f7.

## **References**

- Álvaro, J.J., Ahlberg, P., Loren, B., Bordonaro, O.L., Choi, D.K., et al., 2013, Global Cambrian trilobite palaeobiogeography assessed using parsimony analysis of endemicity: Geological Society, London, Memoirs 38, p. 273–296, https://doi.org/10.1144/M38.19.
- Bagnoli, G., Qi, Y.P., Zuo, J.X., Du, S.X., Liu, S.C., and Zhang, Z.Q. 2014, Integrated biostratigraphy and carbon isotopes from the Cambrian Tangwangzhai section, North China: Palaeoworld, v. 23, p. 112–124.
- Calner, M., Ahlberg, P., Lehnert, O., and Erlström, M., 2013, The lower Palaeozoic of southern Sweden and the Oslo Region, Norway: field guide for the 3rd annual meeting of the IGCP project 591: Sveriges geologiska undersökning Rapporter och meddelanden, v. 133, p. 1–96.
- Cook, H.E., and Taylor, M.E., 1977, Comparison of continental slope and shelf environments in the upper Cambrian and lowest Ordovician of Nevada: Society of Economic Paleontologists and Mineralogists Special Publication, v. 25, p. 51–81, https://doi.org/10.2110/pec.77.25.0051.
- Cook, P.J., and Shergold, J.H., 1984, Phosphorus, phosphorites and skeletal evolution at the Precambrian–Cambrian boundary: *Nature*, v. 308, p. 231–236, https://doi.org/10.1038/308231a0.
- Dong, X., Donoghue, P.C.J., Liu, Z., Liu, J., and Peng, F., 2005, The fossils of Orsten-type preservation from middle and upper Cambrian in Hunan, China: Chinese Science Bulletin, v. 50, p. 1352–1357.
- Dong, X.P., Zhang H. 2017, Middle Cambrian through lowermost Ordovician conodonts from Hunan, South China: *Journal of Paleontology*, v. 91, p. 1–89, https://doi.org/10.1017/jpa.2015.43
- Fortey, R., 2000, Olenid trilobites: the oldest known chemoautotrophic symbionts?: Proceedings of the National Academy of Sciences of the United States of America, v. 97, p. 6574–6578, https://doi.org/10.1073/pnas.97.12.6574.
- Fortey, R., 2014, The palaeoecology of trilobites: *Journal of Zoology*, v. 292, p. 250–259, https://doi.org/10.1111/jzo.12108.
- Gearty, W., 2024, deeptime: plotting tools for anyone working in deep time: R package version 1.1.1, https://CRAN.R-project.org/package=deeptime (accessed May 2025).
- Groom, T., 1902, On Polyphyma, a new genus belonging to the Leperditiadæ, from the Cambrian shales of Malvern: Quarterly Journal of the Geological Society of London, v. 58, no. 229, p. 83–88.
- Gründel, J., and Buchholz, A., 1981, Bradoriida aus kambrischen Geschieben vom Gebiet der nördlichen, DDR: Freiberger Forschungsheft, v. C363, p. 58–73.
- Hinz-Schallreuter, I., 1993, Ostracodes from the middle Cambrian of Australia: Neues Jahrbuch für Geologie und Paläontologie, Abhandlungen, v. 188, p. 305–326.
- Hou, X.G., Siveter, D.J., Williams, M., and Feng, X., 2001, A monograph of the Bradoriid arthropods from the lower Cambrian of SW China: *Transactions of the Royal Society of Edinburgh (Earth Sciences)*, v. 92, p. 347–409, https://doi. org/10.1017/S0263593300000286.
- Huo, J., Shu, D., and Fu, D., 1983, Dabashanella hemicyclica, in Huo, S., Shu, D., Zhang, X., Cui, Z., and Tong, H., 1983, Notes on Cambrian bradoriids from Shaanxi, Yunnan, Sichuan, Guizhou, Hubei and Guangdong: Journal of Northwest University, v. 13, p. 56–75.
- Jones, P.J., and Kruse, P.D., 2009, New middle Cambrian bradoriids (Arthropoda) from the Georgina Basin, Central Australia: Memoirs of the Association of Australasian Palaeontologists, v. 37, p. 55–86.
- Jones, P.J., and Laurie, J., 2006, Bradoriida and Phosphatocopida (Arthropoda) from the Arthur Creek Formation (middle Cambrian), Georgina Basin, central Australia: Memoirs of the Association of Australasian Palaeontologists, v. 32, p. 205–233.
- Judd, E.J., Tierney, J.E., Lunt, D.J., Montañez, I.P., Huber, B.T., Wing, S.L., and Valdes, P.J., 2024, A 485-million-year history of Earth's surface temperature: *Science*, v. 385, n. eadk3705, https://doi.org/10.1126/science.adk3705.
- Kocsis, A.T., Raja, N.B., Williams, S., and Dowding., E.M., 2024, rgplates: R interface for the GPlates Web Service and Desktop Application, https://doi.org/10.5281/zenodo.13711982 (accessed May 2025).
- Kozur, H., 1974, Die Bedeutung der Bradoriida als Vorlaufer der postkambrischen Ostracoden: Zeitschrift der geologischen Wissenschaft Berlin, v. 2, No. 7, p. 823–830.
- Landing, E., and Westrop, S.R., 2015, Late Cambrian (middle Furongian) shallow-marine dysoxic mudstone with calcrete and brachiopod-olenid-

- Lotagnostus faunas in Avalonian Cape Breton Island, Nova Scotia: *Geological Magazine*, v. 152, p. 973–992, https://doi.org/10.1017/S001675681400079X.
- Lankester, R.E., 1904, The structure and classification of the Arthropoda: Quarterly Journal of Microscopical Science, v. 47, p. 523–582, https://doi. org/10.1242/jcs.s2-47.188.523.
- **Lieberman, B.S.**, 2002, Phylogenetic biogeography with and without the fossil record: gauging the effects of extinction and paleontological incompleteness: *Palaeogeography, Palaeoclimatology, Palaeoecology*, **v. 178**, p. 39–52, https://doi.org/10.1016/S0031-0182(01)00367-4.
- Lochman, C., Hu, C.H., 1960, Upper Cambrian faunas from the Wind River Mountains, Wyoming. Part 1: *Journal of paleontology*, v. 34, p. 793–834.
- Maas, A., Waloszek, D., and Muller, K.J., 2003, Morphology, ontogeny, and phylogeny of the Phosphatocopina (Crustacea) from the upper Cambrian "Orsten" of Sweden: *Fossils and Strata*, v. 49, p. 1–244, https://doi.org/10.18261/9781405169875-2003-01.
- Malard, F., and Hervant, F., 1999, Oxygen supply and the adaptations of animals in groundwater: Freshwater Biology, v. 41, p. 1–30, https://doi. org/10.1046/j.1365-2427.1999.00379.x.
- Melnikova, L.M., Siveter, D.J., and Williams, M., 1997, Cambrian Bradoriida and Phophatocopida (Arthropoda) of the former Soviet Union: *Journal of Micropalaeontology*, v. 16, p. 179–191, https://doi.org/10.1144/jm.16.2.179.
- Merdith, A.S., Williams, S.E., Collins, A.S., Tetley, M.G., Mulder, J.A., et al., 2021, Extending full-plate tectonic models into deep time: linking the Neoproterozoic and the Phanerozoic: *Earth-Science Reviews*, v. 214, n. e103477, https://doi.org/10.1016/j.earscirev.2020.103477.
- Miller, J.F., Ripperdan, R.L., Loch, J.D., Freeman, R.L., Evans, K.R., Taylor, J. F., and Tolbart, Z.C., 2015, Proposed GSSP for the base of Cambrian Stage 10 at the lowest occurrence of *Eoconodontus notchpeakensis* in the House Range, Utah, USA: *Annales de Paléontologie*, v. 101, p. 199–211, https://doi.org/10.1016/j.annpal.2015.04.008.
- Müller, K.J., 1964, Ostracoda (Bradorina) mit phosphatischen Gehäusen aus dem Oberkambrium von Schweden: *Neues Jahrbuch für Geologie und Paläontologie*, v. 121, p. 1–46, https://doi.org/10.1111/j.1502-3931.1979.tb01234.x.
- Müller, K.J., 1979, Phosphatocopine ostracodes with preserved appendages from the upper Cambrian of Sweden: *Lethaia*, v. 12, p. 1–27, https://doi. org/10.1111/j.1502-3931.1979.tb01234.x.
- Müller, K.J., 1982, Hesslandona unisulcata sp. nov. with phosphatised appendages from upper Cambrian "Orsten" of Sweden, in Bate, R.H., Robinson, E., and Sheppard, L.M., eds., Fossil and Recent Ostracods: Chichester, Ellis Horwood Limited, p. 276–304.
- Müller, R.D., Cannon, J., Qin, X., Watson, R.J., Gurnis, M., Williams, S., Pfaffelmoser, T., Seton, M., Russell, S.H.J., and Zahirovic, S., 2018, GPlates: building a virtual Earth through deep time: Geochemistry, Geophysics, Geosystems, v. 19, p. 2243–2261, https://doi.org/10.1029/2018GC007584.
- Olempska, E., and Chauffe, K., 1999, Ostracodes of the Maple Mill Shale Formation (Upper Devonian) of Southeastern Iowa, U.S.A: *Micropaleontology*, v. 45, p. 304–318, https://doi.org/10.2307/1486139.
- Olempska, E., Maas, A., Waloszek, D., and Eriksson, M.E., 2019, Exceptionally well-preserved Orsten-type phosphatocopid crustaceans from the Cambrian of Poland: *Acta Palaeontologica Polonic*, v. 6, p. 19–39, https://doi.org/10.4202/app.00553.2018.
- Raja, N.B., Dunne, E.M., Matiwane, A., Khan, T.M., Nätscher, P.S., Ghilardi, A.M., and Chattopadhyay, D., 2022, Colonial history and global economics distort our understanding of deep-time biodiversity: *Nature Ecology and Evolution*, v. 6, p. 145–154, https://doi.org/10.1038/s41559-021-01608-8.
- R Core Team, 2021, R: A Language and Environment for Statistical Computing: Vienna, R Foundation for Statistical Computing.
- Repetski, J.E., Loch, J.D., Taylor, J.F., and Strauss, J.V., 2019, *Lotagnostus* species from the Cambrian (Furongian) Windfall Formation, Nevada, and their significance regarding the GSSP for Cambrian Stage 10: *PaleoBios*, v. 36, n. 5422, https://doi.org/10.11646/zootaxa.5422.1.1.
- Rushton, A.W.A., 1969, Cyclotron, a new name for *Polyphyma* Groom: *Geological Magazine*, v. 106, p. 216–217, https://doi.org/10.1017/S0016756800052055.
- **Rushton, A.W.A.**, 1978, Fossils from the Middle-Upper Cambrian Transition in the Nuneaton District: *Palaeontology*, v. **21**, p. 245–283.
- Scotese, C.R., and Wright, N., 2018, PALEOMAP paleodigital elevation models (PaleoDEMS) for the Phanerozoic: PALEOMAP Project (accessed May 2025).

- Scotese, C.R., Song, H., Mills, B.J.W., and van der Meer, D.G., 2021, Phanerozoic paleotemperatures: the Earth's changing climate during the last 540 million years: *Earth-Science Reviews*, v. 215, n. e103503, https://doi.org/10.1016/j.earscirev.2021.103503.
- Siveter, D.J., Williams, M., and Waloszek, D., 2001, A phosphatocopid crustacean with appendages from the lower Cambrian: *Science*, v. 293, p. 479–481, https://doi.org/10.1126/science.1061697.
- Siveter, D.J., Waloszek, D., and Williams, M., 2003, An early Cambrian phosphatocopid crustacean with three-dimensionally preserved soft parts from Shropshire, England: Special Papers in Palaeontology, v. 70, p. 9–30.
- **Taylor, M.E., and Cook, H.E.,** 1977, Continental shelf and slope facies in the upper Cambrian and lowest Ordovician of Nevada, *in* Cook, H.E., and Enos, P., eds., *Deep-Water Carbonate Environments*: SEPM Special Publication 25.
- Topper, T.P., Skovsted, C.B., Brock, G.A., and Paterson, J.R., 2011, The oldest bivalved arthropods from the early Cambrian of East Gondwana: systematics, biostratigraphy and biogeography: *Gondwana Research*, v. 19, p. 310–326, https://doi.org/10.1016/j.gr.2010.05.012.
- **Torsvik, T.H., and Cocks, L.R.M.**, 2016, *Earth History and Palaeogeography*: Cambridge, Cambridge University Press, 317 p.
- **Tortello**, M.F., 2014, A systematic revision of the late Furongian trilobites from Cerro Pelado, Mendoza, Argentina: *Ameghiniana*, v. 51, p. 295–310, https://doi.org/10.5710/AMGH.28.05.2014.2714.
- Valetich, M., Zivak, D., Spandler, C., Degeling, H., and Grigorescu, M., 2022, REE enrichment of phosphorites: an example of the Cambrian Georgina Basin of Australia: *Chemical Geology*, v. 588, n. e120654, https://doi.org/ 10.1016/j.chemgeo.2021.120654.
- Walossek, D., Hinz-Schallreuter, I., Shergold, J.H., and Müller, K.J., 1993, Three-dimensional preservation of arthropod integument from the middle Cambrian of Australia: *Lethaia*, v. 26, p. 7–15, https://doi.org/10.1111/j.1502-3931.1993.tb01504.x.
- Westrop, S.R., Adrain, J.M., and Landing, E., 2011, The Cambrian (Sunwaptan, Furongian) agnostoid arthropod *Lotagnostus* Whitehouse, 1936, in Laurentian and Avalonian North America: systematics and biostratigraphic significance: *Bulletin of Geosciences*, v. 86, p. 569–594, https://doi. org/10.3140/bull.geosci.1256.
- Williams, M., and Siveter, D.J., 1998, British Cambrian and Tremadoc bradoriid and phosphatocopid arthropods: Monograph of the Palaeontographical Society, v. 152, p. 1–61, https://doi.org/10.1080/25761900.1998.12288893.
- Williams, M., Siveter, D.J., Rushton, A.W.A., and Berg-Madsen, V., 1994, The upper Cambrian bradoriid ostracod *Cyclotron lapworthi* is a

- hesslandonid: Transactions of the Royal Society of Edinburgh: *Earth Sciences*, v. 85, p. 123–130, https://doi.org/10.1017/S0263593300003527.
- Williams, M., Siveter, D.J., Popov, L.E., and Vannier, J.M.C., 2007, Biogeography and affinities of the bradoriid arthropods: cosmopolitan microbenthos of the Cambrian seas: *Palaeogeography, Palaeoclimatology, Palaeoecology*, v. 248, p. 202–232, https://doi.org/10.1016/j.palaeo.2006.12.004.
- Williams, M., Vannier, J., Corbari, L., and Massabuau, J.-C., 2011, Oxygen as a driver of early arthropod micro-benthos evolution: *PLoS ONE*, v. 6, n. e28183, https://doi.org/10.1371/journal.pone.0028183.
- Wrona, R., 2009, Early Cambrian bradoriide and phosphatocopide arthropods from King George Island, West Antarctica: biogeographic implications: Polish Polar Research, v. 30, p. 347–377.
- Zhai, D., Williams, M., Siveter, D.J., Harvey, T.H.P., Sansom, R.S., Gabbott, S.E., Ma, X., Zhou, R., Liu, Y., and Hou, X., 2019, Variation in appendages in early Cambrian bradoriids reveals a wide range of body plans in stemeuarthropods: Communications Biology, v. 2, p. 1–6, https://doi.org/10.1038/s42003-019-0573-5.
- Zhang, C., Guan, S., Wu, L., Ren, R., Wang, L., and Wu, Z., 2020, Depositional environments of early Cambrian marine shale, northwestern Tarim Basin, China: implications for organic matter accumulation: *Journal of Petroleum Science and Engineering*, v. 194, n. e107497, https://doi.org/10.1016/j.petrol.2020.107497.
- Zhang, H., and Dong, X., 2009, Two new species of *Vestrogothia* (Phosphatocopina, Crustacea) of Orsten-type preservation from the upper Cambrian in western Hunan, South China: *Science in China Series D Earth Science*, v. 52, p. 784–796, https://doi.org/10.1007/s11430-009-0069-0.
- **Zhang, H., Dong, X., and Xiao, S.,** 2011, Two species of Hesslandona (Phosphatocopida, Crustacea) from the upper Cambrian of Western Hunan, South China and the phylogeny of Phosphatocopida: *Journal of Paleontology*, **v. 85**, p. 770–788, https://doi.org/10.1666/10-043.1.
- Zhang, H., Dong, X., and Xiao, S., 2012, Three head-larvae of Hesslandona angustata (Phosphatocopida, Crustacea) from the upper Cambrian of Western Hunan, South China, and the phylogeny of Crustacea: Gondwana Research, v. 21, p. 1115–1127, https://doi.org/10.1016/j.gr.2011.07.003.
- Zhang, X., and Pratt, B.R., 2012, The first stalk eyed phosphatocopine crustacean from the lower Cambrian of China: Current Biology, v. 22, p. 2149–2154, https://doi.org/10.1016/j.cub.2012.09.027.
- Zrzavý, J., and Štys, P., 1997, The basic body plan of arthropods: insights from evolutionary morphology and developmental biology: *Journal of Evolutionary Biology*, v. 10, p. 353–367, https://doi.org/10.1046/j.1420-9101.1997.10030353.x.